Exact analytical solution for free axisymmetric and non-axisymmetric vibrations of FGM porous circular plates

Krzysztof Kamil Żur*, Piotr Jankowski

Faculty of Engineering Management
Bialystok University of Technology
Ojca Stefana Tarasiuka 2
16-001 Kleosin, Poland
*Corresponding Author: k.zur@pb.edu.pl

Abstract

Free vibration analysis of the porous functionally graded circular plates has been presented on the basis of classical plate theory. The three defined coupled equations of motion of the porous functionally graded circular/annular plate were decoupled to one differential equation of free transverse vibrations of plate. The one universal general solution was obtained as linear combination of the multiparametric special functions for the functionally graded circular and annular plates with even and uneven porosity distributions. The multiparametric frequency equations of functionally graded porous circular plate with diverse boundary conditions were obtained in the exact closed-form. The influences of the even and uneven distributions of porosity, power-law index, diverse boundary conditions and the negligibled effect of the coupling in-plane and transverse displacements on the dimensionless frequencies of the circular plate were comprehensively studied for the first time. The formulated boundary value problem, the exact method of solution and the numerical results for the perfect and imperfect functionally graded circular plates have not yet been reported.

Keywords: FGM porous circular plate, Free vibration, Exact solution, Multiparametric frequency equations.

1. Introduction

Functionally graded materials (FGMs) are a class of composite materials, which are made of the ceramic and metal mixture such that the material properties vary continuously in appropriate directions of structural components. In the processes of preparing functionally graded material, micro-voids and porosities may appear inside material in view of the technical issues. Zhu et al. [1] reported that many porosities appear in material during the functionally graded material preparation process by the non-pressure sintering technique. Wattanasakulpong et al. [2] reported that exist many porosities in the intermediate area of the functionally graded material fabricated by utilizing multi-step sequential infiltration technique because of the problem with infiltration of the secondary material into the middle area. In that case less porosities appear in the top and bottom area of material because infiltration of the material is easier in these zones.

In recent years, a significant number of articles about the free vibrations of porous functionally graded (FGM) plates have appeared in the literature due to their wide applications in many fields of engineering such us aeronautical, civil, mechanical, automotive, and ocean engineering. The gradation of properties in functionally graded materials and the diverse distributions of porosity have a significant effect on distributions of the mass and the stiffness of plates and therefore their natural frequencies. The knowledge about influence of distribution of the material properties on dynamics of plates is very important because allows us to predict the frequency of plates and find their optimal parameters. Additionally, the comprehensive investigation of the effect of functionally graded material with

porosities and diverse boundary conditions on the natural frequencies of plates is the first important step to design of their safe and rational active vibration control system.

We note that in most engineering applications, the classical plate theory is often used to analysis of the dynamic behavior of thin lightweight plates. It is impossible to review all works focused on mechanical behavior of porous FGM structures, then we limit to chronological reviewing some of the works focused on mechanical behavior of porous and porous FGM plates that are closely related to our work.

Jabbari et al. [3] studied the buckling of thin saturated porous circular plate with the layers of piezoelectric actuators. Buckling load was obtained for clamped circular plate under uniform radial compressive loading. The same authors presented the buckling analysis of clamped thin saturated porous circular plate with sensor-actuator layers under uniform radial compression [4]. Mojahedin et al. [5] investigated thermal and mechanical stability of clamped thin saturated and unsaturated porous circular plate with piezoelectric actuators. Rad and Shariyat [6] solved to three-dimensional magneto-elastic problem for asymmetric variable thickness porous FGM circular supported on the Kerr elastic foundation using the differential quadrature method and the state space vector technique. Barati et al. [7] studied buckling of functionally graded piezoelectric rectangular plates with porosities based on the four-variable plate theory. Mechab et al. [8] studied free vibration of FGM nanoplate with porosities resting on Winkler and Pasternak elastic foundation based on the two-variable plate theory. Mojahedin et al. [9] analyzed buckling of radially loaded clamped saturated porous circular plates based on higher order shear deformation theory. Wang and Zu [10] analyzed vibration behaviors of thin FGM rectangular plates with porosities and moving in thermal environment using the method of harmonic balance and the Runge-Kutta technique. Gupta and Talha [11] analyzed flexural and vibration response of porous FGM rectangular plates using nonpolynomial higher-order shear and normal deformation theory. Wang and Zu [12] analyzed vibration characteristics of longitudinally moving sigmoid porous FGM plates based on the von Kármán non-linear plate theory. Ebrahimi et al. [13] studied free vibration of smart shear deformable rectangular plates made of porous magneto-electro-elastic functionally graded materials. Feyzi and Khorshidvand [14] studied axisymmetric pos-buckling behavior of a saturated porous circular plate with simply supported and clamped boundary conditions. Wang and Zu [15] studied large-amplitude vibration of thin sigmoid functionally graded plates with porosities. Wang et al. [16] studied vibrations of longitudinally travelling FGM porous thin rectangular plates using the Galerkin method and the four-order Runge-Kutta method. Ebrahimi et al. [17] used a four-variable shear deformation refined plate theory for free vibration analysis of embedded smart rectangular plates made of magneto-electro-elastic porous functionally graded materials. Shahverdi and Barati [18] developed nonlocal strain-gradient elasticity model for vibration analysis of porous FGM nano-scale rectangular plates. Shojaeefard et al. [19] studied free vibration and thermal buckling of micro temperature-dependent FGM porous circular plate using the generalized differential quadrature method. Barati and Shahverdi [20] presented new solution to examine large amplitude vibration of a porous nanoplate resting on a nonlinear elastic foundation modeled by nonlinear the four-variable plate theory. Kiran et al. [21] studied free vibration of porous FGM magneto-electro-elastic skew plates using the finite element formulation. Cong et al. [22] presented analytical approach to buckling and post-buckling behavior analysis of FGM rectangular plates with porosities under thermal and thermomechanical loads based on the Reddy's higher-order shear deformation theory. Kiran and Kattimani [23] studied free vibration and static behavior of porous FGM magneto-electro-elastic rectangular plates using the finite element method. Arshid and Khorshidvand [24] analyzed free vibration of saturated porous FGM circular plates integrated with piezoelectric actuators using the differential quadrature method. Shahsavari et al. [25] used the quasi-3D hyperbolic theory for free vibration of porous FGM rectangular plates resting on Winkler, Pasternak and Kerr foundations.

2. Present study

The aim of the paper is to formulate and solve the boundary value problem for the free axisymmetric and non-axisymmetric vibrations of FGM circular plate with even and uneven porosity distributions and diverse boundary conditions. The defined coupled equations of motion for the porous FGM circular plate were decoupled based on the properties of physical neutral surface. The general solution of the decoupled equation of motion of porous FGM circular plate was defined as the linear combination of the Bessel functions functionally dependent on the material parameters. The obtained characteristic equations allow us to comprehensively study the effect of the distribution of material parameters and the formulated boundary conditions on the natural frequencies of axisymmetric and non-axisymmetric vibrations of the circular plates without necessity to solve to new eigenvalue problem for plates with steady distribution of parameters.

Authors of many previous papers (e.g. [27], [28], [29], [30]) presented the free vibration analysis of the perfect (without porosity) FGM circular plates using the equation of motion including only the coefficient of the pure bending stiffness varying in the thickness direction of the plate. The coefficients of the extensional stiffness and the bending-extensional coupling stiffness were neglected because the effect of the coupled in-plane and transverse displacements was omitted for obtaining simplified solution to the eigenvalue problem.

In the present paper the obtained equation of motion of the perfect and imperfect FGM circular plates includes the coefficients of extensional stiffness, bending-extensional coupling stiffness and bending stiffness, which appeared by decoupling the in-plane and transverse displacements using the properties of the physical neutral surface. The differences between the values of numerical results for the eigenfrequencies of the perfect FGM circular plate with and without the coupling effect are shown for diverse boundary conditions.

A review of literature shows that there are no studies which focus on the free axisymmetric and non-axisymmetric vibrations of FGM and porous FGM circular plates. In particular, the obtained exact solution, the multiparametric frequency equations and the calculated eigenfrequencies for the free vibrations of perfect and imperfect FGM circular plates with clamped, simply supported, sliding and free edges have not yet been reported. The present paper fills this void in the literature.

3. FGM circular plate with porosities

Consider a porous FGM thin circular plate with radius R and thickness h presented in the cylindrical coordinate (r, θ, z) with the z-axis along the longitudinal direction. The geometry and the coordinate system of the considered circular plate are shown in Fig. 1. The FGM plate contains evenly (e) and unevenly (u) distributed porosities along the plate's thickness direction. The cross-sections of the FGM circular plates with the two various types of distribution of porosities are shown in Fig. 2.

The functionally graded material is a mixture of a ceramic (c) and a metal (m). If the volume fraction of the ceramic part is V_c and the metallic part is V_m, we have the well-known dependence [31]:

$$V_c(z) + V_m(z) = 1. \tag{1}$$

Based on the modified rule of mixtures [16] with the porosity volume fraction ψ ($\psi \ll 1$), the Young's modulus, the density and the Poisson's ratio for evenly (e) distributed porosities over the cross-section of the plate have the general forms:

$$E^e(z, \psi) = E_c \left[V_c(z) - \frac{\psi}{2} \right] + E_m \left[V_m(z) - \frac{\psi}{2} \right], \tag{2a}$$

$$\rho^e(z, \psi) = \rho_c \left[V_c(z) - \frac{\psi}{2} \right] + \rho_m \left[V_m(z) - \frac{\psi}{2} \right], \tag{2b}$$

$$\nu^e(z, \psi) = \nu_c \left[V_c(z) - \frac{\psi}{2} \right] + \nu_m \left[V_m(z) - \frac{\psi}{2} \right]. \tag{2c}$$
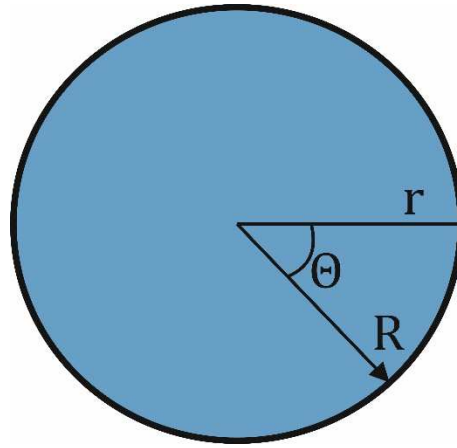
Fig. 1. The geometry and the coordinate system of the porous FGM circular plate.
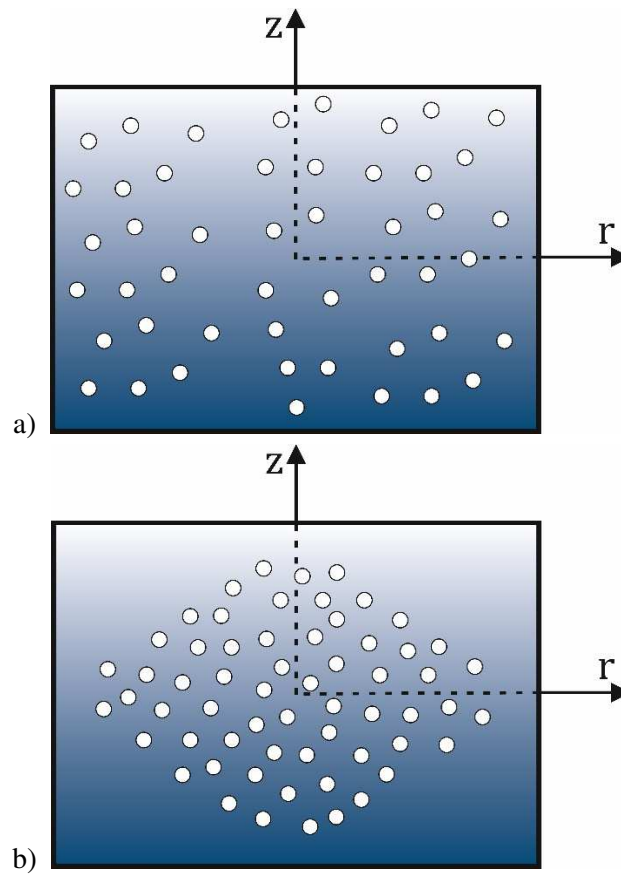
Fig. 2. The cross-sections of the porous FGM circular plate: a) even distribution; b) uneven distribution.

The volume fraction of the ceramic part changes continually along the thickness and can be defined as [32]

$$V_c(z,g) = \left(\frac{z}{h} + \frac{1}{2}\right)^g, \quad g \geq 0, \tag{3}$$

where g is the power-law index of the material. A change in the power g of functionally graded material results in a change in the portion of the ceramic and metal components in the circular plate. We assume that the composition is varied from the bottom surface $(z = -h/2)$ to the top surface $(z = h/2)$ of the circular plate. After substituting the variation of the ceramic part $V_c(z,g)$ from Eq. (3) into Eqs. (2), the

material properties of the functionally graded circular plate with evenly distributed porosities are defined in the final form:

$$E^e(z, g, \psi) = (E_c - E_m)\left(\frac{z}{h} + \frac{1}{2}\right)^g + E_m - \frac{\psi}{2}(E_c + E_m),$$ (4a)

$$\rho^e(z, g, \psi) = (\rho_c - \rho_m)\left(\frac{z}{h} + \frac{1}{2}\right)^g + \rho_m - \frac{\psi}{2}(\rho_c + \rho_m),$$ (4b)

$$\nu^e(z, g, \psi) = (\nu_c - \nu_m)\left(\frac{z}{h} + \frac{1}{2}\right)^g + \nu_m - \frac{\psi}{2}(\nu_c + \nu_m).$$ (4c)

For the functionally graded circular plate with unevenly (*u*) distributed porosities [16], the material properties in Eqs. (4) can be replaced by the following forms:

$$E^u(z, g, \psi) = (E_c - E_m)\left(\frac{z}{h} + \frac{1}{2}\right)^g + E_m - \frac{\psi}{2}(E_c + E_m)\left(1 - \frac{2|z|}{h}\right),$$ (5a)

$$\rho^u(z, g, \psi) = (\rho_c - \rho_m)\left(\frac{z}{h} + \frac{1}{2}\right)^g + \rho_m - \frac{\psi}{2}(\rho_c + \rho_m)\left(1 - \frac{2|z|}{h}\right),$$ (5b)

$$\nu^u(z, g, \psi) = (\nu_c - \nu_m)\left(\frac{z}{h} + \frac{1}{2}\right)^g + \nu_m - \frac{\psi}{2}(\nu_c + \nu_m)\left(1 - \frac{2|z|}{h}\right).$$ (5c)

In this case the porosity linearly decrease to zero at the top and the bottom of the cross-section of the plate. The effect of Poisson's ratio is much less on the mechanical behavior of FGM plates [33, 34] than the Young's modulus, thus the Poisson's ratio will assume to be constant $\nu^e = \nu^u = \nu$ in the whole volume of the porous FGM circular plate.

4. Constitutive relations and governing equations

In most practical applications, the ratio of the radius R to the thickness h of the plate is more than 10, then the assumptions of classical plate theory (CPT) are applicable and rotary inertia and shear deformation can be successfully omitted.

For a thin circular plate, the displacement field has the form:

$$u_r(r, \theta, z, t) = u(r, \theta, t) - z\frac{\partial w(r, \theta, t)}{\partial r},$$ (6a)

$$u_\theta(r, \theta, z, t) = v(r, \theta, t) - \frac{z}{r}\frac{\partial w(r, \theta, t)}{\partial \theta},$$ (6b)

$$w(r, \theta, z, t) = w(r, \theta, t),$$ (6c)

where u, v and w are the radial, circumferential and transverse displacements of the midplane ($z = 0$) of the plate at time t. Based on the linear strain-displacement relations and Hook's law, the resultant forces and the moments for porous FGM circular plate ($i = \{e, u\}$) can be expressed in the following form [35]:

$$\begin{pmatrix} N_{rr}^i \\ N_{\theta\theta}^i \\ N_{r\theta}^i \end{pmatrix} = \begin{bmatrix} A_{11}^i & A_{12}^i & 0 \\ A_{12}^i & A_{11}^i & 0 \\ 0 & 0 & A_{33}^i \end{bmatrix} \begin{pmatrix} \varepsilon_{rr}^0 \\ \varepsilon_{\theta\theta}^0 \\ \gamma_{r\theta}^0 \end{pmatrix} + \begin{bmatrix} B_{11}^i & B_{12}^i & 0 \\ B_{12}^i & B_{11}^i & 0 \\ 0 & 0 & B_{33}^i \end{bmatrix} \begin{pmatrix} \kappa_{rr} \\ \kappa_{\theta\theta} \\ \kappa_{r\theta} \end{pmatrix},$$ (7a)

$$\begin{pmatrix} M_{rr}^i \\ M_{\theta\theta}^i \\ M_{r\theta}^i \end{pmatrix} = \begin{bmatrix} B_{11}^i & B_{12}^i & 0 \\ B_{12}^i & B_{11}^i & 0 \\ 0 & 0 & B_{33}^i \end{bmatrix} \begin{pmatrix} \varepsilon_{rr}^0 \\ \varepsilon_{\theta\theta}^0 \\ \gamma_{r\theta}^0 \end{pmatrix} + \begin{bmatrix} D_{11}^i & D_{12}^i & 0 \\ D_{12}^i & D_{11}^i & 0 \\ 0 & 0 & D_{33}^i \end{bmatrix} \begin{pmatrix} \kappa_{rr} \\ \kappa_{\theta\theta} \\ \kappa_{r\theta} \end{pmatrix},$$ (7b)

where

$$\left(\varepsilon_{rr}^0, \varepsilon_{\theta\theta}^0, \gamma_{r\theta}^0\right) = \left(\frac{\partial u}{\partial r}, \frac{1}{r}\frac{\partial v}{\partial \theta} + \frac{u}{r}, \frac{1}{r}\frac{\partial u}{\partial \theta} + \frac{\partial v}{\partial r} - \frac{v}{r}\right),$$ (8a)

$$(\kappa_{rr}, \kappa_{\theta\theta}, \kappa_{r\theta}) = \left(-\frac{\partial^2 w}{\partial r^2}, -\frac{1}{r^2}\frac{\partial^2 w}{\partial \theta^2} - \frac{1}{r}\frac{\partial w}{\partial r}, -\frac{2}{r}\frac{\partial^2 w}{\partial r\partial \theta} + \frac{2}{r^2}\frac{\partial w}{\partial \theta}\right)$$ (8b)

are the in-plane strains and curvatures of midplane, respectively.

We assume that the material properties are varied from the bottom surface ($z = -h/2$) to the top surface ($z = h/2$) of the plate, then the coefficients of extensional stiffness A_{kl}^i, bending-extensional coupling stiffness B_{kl}^i and bending stiffness D_{kl}^i can be defined for FGM circular plate with *i-th* distribution of porosities in the general forms:

$$\left(A_{11}^i, B_{11}^i, D_{11}^i\right) = \int_{-h/2}^{h/2} \frac{E^i(z,g,\psi)}{1-v^2}(1,z,z^2)dz, \tag{9a}$$

$$\left(A_{12}^i, B_{12}^i, D_{12}^i\right) = \int_{-h/2}^{h/2} \frac{vE^i(z,g,\psi)}{1-v^2}(1,z,z^2)dz, \tag{9b}$$

$$\left(A_{33}^i, B_{33}^i, D_{33}^i\right) = \int_{-h/2}^{h/2} \frac{E^i(z,g,\psi)}{2(1+v)}(1,z,z^2)dz. \tag{9c}$$

Additionally, the stiffness coefficients from Eqs. (9) satisfy the equations

$$A_{12}^i + 2A_{33}^i = A_{11}^i, \quad B_{12}^i + 2B_{33}^i = B_{11}^i, \quad D_{12}^i + 2D_{33}^i = D_{11}^i. \tag{10}$$

The resultant forces and the moments can be also defined by

$$\left(N_{rr}^i, N_{\theta\theta}^i, N_{r\theta}^i\right) = \int_{-h/2}^{h/2} \left(\sigma_{rr}^i, \sigma_{\theta\theta}^i, \tau_{r\theta}^i\right)dz, \tag{11a}$$

$$\left(M_{rr}^i, M_{\theta\theta}^i, M_{r\theta}^i\right) = \int_{-h/2}^{h/2} \left(\sigma_{rr}^i z, \sigma_{\theta\theta}^i z, \tau_{r\theta}^i z\right)dz, \tag{11b}$$

where the stress components and the strain components have the form:

$$\begin{pmatrix} \sigma_{rr}^i \\ \sigma_{\theta\theta}^i \\ \tau_{r\theta}^i \end{pmatrix} = \begin{pmatrix} \frac{E^i(z,g,\psi)}{1-v^2}(\varepsilon_{rr} + v\varepsilon_{\theta\theta}) \\ \frac{E^i(z,g,\psi)}{1-v^2}(\varepsilon_{\theta\theta} + v\varepsilon_{rr}) \\ \frac{E^i(z,g,\psi)}{2(1+v)}(2\gamma_{r\theta}) \end{pmatrix}, \tag{12}$$

$$\begin{pmatrix} \varepsilon_{rr} \\ \varepsilon_{\theta\theta} \\ 2\gamma_{r\theta} \end{pmatrix} = \begin{pmatrix} \varepsilon_{rr}^0 + z\kappa_{rr} \\ \varepsilon_{\theta\theta}^0 + z\kappa_{\theta\theta} \\ \gamma_{r\theta}^0 + z\kappa_{r\theta} \end{pmatrix}. \tag{13}$$

4.1. Coupled equations of motion

Using the Hamilton's principle [35] and ignoring in-plane inertia forces, the equilibrium equations of motion of the porous FGM thin circular plate have the forms:

$$\frac{\partial N_{rr}^i}{\partial r} + \frac{1}{r}\left(\frac{\partial N_{r\theta}^i}{\partial \theta} + N_{rr}^i - N_{\theta\theta}^i\right) = 0, \tag{14a}$$

$$\frac{\partial N_{r\theta}^i}{\partial r} + \frac{1}{r}\frac{\partial N_{\theta\theta}^i}{\partial \theta} + \frac{2}{r}N_{r\theta}^i = 0, \tag{14b}$$

$$\frac{\partial^2 M_{rr}^i}{\partial r^2} + \frac{2}{r}\frac{\partial M_{rr}^i}{\partial r} + \frac{1}{r^2}\frac{\partial^2 M_{\theta\theta}^i}{\partial \theta^2} - \frac{1}{r}\frac{\partial M_{\theta\theta}^i}{\partial r} + \frac{2}{r}\frac{\partial^2 M_{r\theta}^i}{\partial r\partial \theta} + \frac{2}{r^2}\frac{\partial M_{r\theta}^i}{\partial \theta} = \rho^i h \frac{\partial^2 w}{\partial t^2}, \tag{14c}$$

where the resultants forces and the moments can be obtain using Eqs. (7) and (8), and can be presented in the following form:

$$N_{rr}^i = A_{11}^i \frac{\partial u}{\partial r} + A_{12}^i\left(\frac{1}{r}\frac{\partial v}{\partial \theta} + \frac{u}{r}\right) - B_{11}^i \frac{\partial^2 w}{\partial r^2} - B_{12}^i\left(\frac{1}{r^2}\frac{\partial^2 w}{\partial \theta^2} + \frac{1}{r}\frac{\partial w}{\partial r}\right), \tag{15a}$$

$$N_{\theta\theta}^i = A_{12}^i \frac{\partial u}{\partial r} + A_{11}^i\left(\frac{1}{r}\frac{\partial v}{\partial \theta} + \frac{u}{r}\right) - B_{12}^i \frac{\partial^2 w}{\partial r^2} - B_{11}^i\left(\frac{1}{r^2}\frac{\partial^2 w}{\partial \theta^2} + \frac{1}{r}\frac{\partial w}{\partial r}\right), \tag{15b}$$

$$N_{r\theta}^i = A_{33}^i\left(\frac{1}{r}\frac{\partial u}{\partial \theta} + \frac{\partial v}{\partial r} - \frac{v}{r}\right) - B_{33}^i\left(\frac{2}{r}\frac{\partial^2 w}{\partial r\partial \theta} - \frac{2}{r^2}\frac{\partial w}{\partial \theta}\right), \tag{15c}$$

$$M_{rr}^i = B_{11}^i \frac{\partial u}{\partial r} + B_{12}\left(\frac{1}{r}\frac{\partial v}{\partial \theta} + \frac{u}{r}\right) - D_{11}^i \frac{\partial^2 w}{\partial r^2} - D_{12}^i\left(\frac{1}{r^2}\frac{\partial^2 w}{\partial \theta^2} + \frac{1}{r}\frac{\partial w}{\partial r}\right), \tag{16a}$$

$$M_{\theta\theta}^i = B_{12}^i \frac{\partial u}{\partial r} + B_{11}^i\left(\frac{1}{r}\frac{\partial v}{\partial \theta} + \frac{u}{r}\right) - D_{12}^i \frac{\partial^2 w}{\partial r^2} - D_{11}^i\left(\frac{1}{r^2}\frac{\partial^2 w}{\partial \theta^2} + \frac{1}{r}\frac{\partial w}{\partial r}\right), \tag{16b}$$

$$M_{r\theta}^i = B_{33}^i \left(\frac{1}{r}\frac{\partial u}{\partial \theta} + \frac{\partial v}{\partial r} - \frac{v}{r}\right) - D_{33}^i \left(\frac{2}{r}\frac{\partial^2 w}{\partial r \partial \theta} - \frac{2}{r^2}\frac{\partial w}{\partial \theta}\right). \tag{16c}$$

In Eq. (14c) ρ^i is the averaged material density of the FGM circular plate for the *i-th* distribution of porosities presented in the general form:

$$\rho^i \equiv \rho^i(g,\psi) = \frac{1}{h}\int_{-h/2}^{h/2}\rho^i(z,g,\psi)dz, \quad i = \{e,u\}. \tag{17}$$

Substituting Eqs. (15) and Eqs. (16) into Eqs. (14), and using relations given in Eq. (10), we get the coupled equilibrium equations of motion of the porous FGM circular plate presented in terms of displacement components:

$$A_{11}^i \left(\frac{\partial^2 u}{\partial r^2} + \frac{1}{r}\frac{\partial u}{\partial r} - \frac{u}{r^2} - \frac{1}{r^2}\frac{\partial v}{\partial \theta} + \frac{1}{r}\frac{\partial^2 v}{\partial r \partial \theta}\right) + A_{33}^i \left(\frac{1}{r^2}\frac{\partial^2 u}{\partial \theta^2} - \frac{1}{r}\frac{\partial^2 v}{\partial r \partial \theta} - \frac{1}{r^2}\frac{\partial v}{\partial \theta}\right) - B_{11}^i \frac{\partial \nabla^2 w}{\partial r} = 0, \tag{18a}$$

$$A_{11}^i \left(\frac{1}{r^2}\frac{\partial u}{\partial \theta} + \frac{1}{r}\frac{\partial^2 u}{\partial r \partial \theta} + \frac{1}{r^2}\frac{\partial^2 v}{\partial \theta^2}\right) + A_{33}^i \left(\frac{1}{r^2}\frac{\partial u}{\partial \theta} - \frac{1}{r}\frac{\partial^2 u}{\partial r \partial \theta} + \frac{\partial^2 v}{\partial r^2} + \frac{1}{r}\frac{\partial v}{\partial r} - \frac{v^2}{r}\right) - B_{11}^i \frac{1}{r}\frac{\partial \nabla^2 w}{\partial \theta} = 0, \tag{18b}$$

$$D_{11}^i \nabla^2 \nabla^2 w - B_{11}^i \nabla^2 \varepsilon = -\rho^i h \frac{\partial^2 w}{\partial t^2}, \tag{18c}$$

where $\nabla^2 = \frac{\partial^2}{\partial r^2} + \frac{1}{r}\frac{\partial}{\partial r} + \frac{1}{r^2}\frac{\partial^2}{\partial \theta^2}$ is the Laplace operator presented in polar coordinates and

$$\varepsilon = \frac{\partial u}{\partial r} + \frac{1}{r}\frac{\partial v}{\partial \theta} + \frac{u}{r}. \tag{19}$$

4.2. Decoupled equation of motion

Eqs. (18) show, that the in-plane stretching and bending are coupled because the reference surface is a geometrical midplane. We can eliminate this coupling by introducing the physical neutral surface [26], where the in-plane displacements will be omitted. The in-plane displacements of the midplane can be expressed in terms of the slopes of deflection in the following form:

$$u(r,\theta,t) = z_0 \frac{\partial w(r,\theta,t)}{\partial r}, \tag{20a}$$

$$v(r,\theta,t) = z_0 \frac{1}{r}\frac{\partial w(r,\theta,t)}{\partial \theta}, \tag{20b}$$

where z_0 is the distance between the midplane and the physical neutral surface. By substituting Eqs. (20) into Eqs. (6) and Eqs. (15) and introducing $z = z_0$, the in-plane displacements u, v and the in-plane forces N_{rr}^i, $N_{\theta\theta}^i$, $N_{r\theta}^i$ must equal zero based on properties of the physical neutral surface. By substituting Eqs. (20) into Eqs. (15)

$$N_{rr}^i = \left(z_0 A_{11}^i - B_{11}^i\right)\frac{\partial^2 w}{\partial r^2} + \left(z_0 A_{12}^i - B_{12}^i\right)\left(\frac{1}{r^2}\frac{\partial^2 w}{\partial \theta^2} + \frac{1}{r}\frac{\partial w}{\partial r}\right) = 0, \tag{21a}$$

$$N_{\theta\theta}^i = \left(z_0 A_{12}^i - B_{12}^i\right)\frac{\partial^2 w}{\partial r^2} + \left(z_0 A_{11}^i - B_{11}^i\right)\left(\frac{1}{r^2}\frac{\partial^2 w}{\partial \theta^2} + \frac{1}{r}\frac{\partial w}{\partial r}\right) = 0, \tag{21b}$$

$$N_{r\theta}^i = \left(z_0 A_{33}^i - B_{33}^i\right)\left(\frac{2}{r}\frac{\partial^2 w}{\partial r \partial \theta} - \frac{2}{r^2}\frac{\partial w}{\partial \theta}\right) = 0 \tag{21c}$$

and assuming that the Poisson's ratio is constant, distance z_0 can be obtained from relations:

$$z_0 A_{11}^i - B_{11}^i = z_0 A_{12}^i - B_{12}^i = z_0 A_{33}^i - B_{33}^i = 0, \tag{22}$$

where

$$z_0 = \frac{B_{11}^i}{A_{11}^i} = \frac{B_{12}^i}{A_{12}^i} = \frac{B_{33}^i}{A_{33}^i} = \frac{\int_{-h/2}^{h/2} E^i(z,g,\psi)z\,dz}{\int_{-h/2}^{h/2} E^i(z,g,\psi)dz}. \tag{23}$$

By substituting Eqs. (20) and Eq. (23) into Eq. (19) and Eq. (18c), we obtain the decoupled equation of transverse vibration of the porous FGM thin circular plate in the form:

$$\mathfrak{D}^i \nabla^2 \nabla^2 w = -\rho^i h \frac{\partial^2 w}{\partial t^2}; \tag{24}$$

where

$$\mathfrak{D}^i = D_{11}^i - \frac{\left(B_{11}^i\right)^2}{A_{11}^i}. \tag{25}$$

5. Formulation of the problem

For a harmonic solution, the non-axisymmetric deflection of the porous FGM circular plate may be expressed as follows:

$$w(r,\theta,t) = W(r)\cos(n\theta)\cos(\omega t), \tag{26}$$

where $W(r)$ is the radial mode function as the small deflection compared with the thickness h of the plate, n is the integer number of diagonal nodal lines, θ is the angular coordinate, ω is the natural frequency. By substituting Eq. (26) into Eq. (24) using the dimensionless coordinate $\xi = r/R$ $(0 < \xi \le 1)$, the general governing differential equation assumes the following form:

$$\mathcal{L}_n(W) = \rho^i h \omega^2 W \tag{27}$$

where $\mathcal{L}_n(\cdot)$ is the differential operator defined by

$$\mathcal{L}_n(\cdot) \equiv \mathfrak{D}^i \frac{d^4}{d\xi^4} + \frac{2\mathfrak{D}^i}{\xi}\frac{d^3}{d\xi^3} - \frac{(1+2n^2)\mathfrak{D}^i}{\xi^2}\frac{d^2}{d\xi^2} + \frac{(1+2n^2)\mathfrak{D}^i}{\xi^3}\frac{d}{d\xi} + \frac{(n^4-4n^2)\mathfrak{D}^i}{\xi^4}. \tag{28}$$

The calculated general forms of material density ρ^i and the coefficients of extensional stiffness $\left(A_{11}^i\right)$, extensional-bending coupling stiffness $\left(B_{11}^i\right)$ and bending stiffness $\left(D_{11}^i\right)$ for the porous FGM circular plate are presented in the following general forms:

$$\rho^i = \frac{\rho_c(2x-\psi-g\psi)+\rho_m(2xg-\psi-\psi g)}{2x(1+g)}, \tag{29a}$$

$$A_{11}^i = \frac{E_c h}{1-\nu^2}\left[\frac{(2x-\psi-g\psi)+\frac{E_m}{E_c}(2xg-\psi-g\psi)}{2x(1+g)}\right], \tag{29b}$$

$$B_{11}^e = B_{11}^u = \frac{E_c h^2}{(1-\nu^2)}\left[\frac{g(1-\frac{E_m}{E_c})}{2(1+g)(2+g)}\right], \tag{29c}$$

$$D^i = \frac{E_c h^3}{12(1-\nu^2)}\left[\frac{\psi(6g^2+6g+12)-\psi(1+g)(2+g)(3+g)+\frac{E_m}{E_c}[\psi(2g^3+6g^2+16g)-\psi(1+g)(2+g)(3+g)]}{2\psi(1+g)(2+g)(3+g)}\right], \tag{29d}$$

where $x = \psi = 1$ for the even distribution $(i = e)$ of porosities and $x = 2$, $\psi = 4$ for the uneven $(i = u)$ distribution of porosities. The extensional-bending coupling stiffness B_{11}^i have the same form for both types of porosities.

By substituting the obtained forms from Eqs. (29) into Eq. (27), the generalized ordinary differential equation with variable coefficients is obtained as:

$$\mathcal{L}_n(W)_\chi = \lambda^2 \mu^i W, \tag{30}$$

where

$$\mathcal{L}_n(\cdot)_\chi \equiv \left(\chi_1^i + \chi_2^i\right)\frac{d^4}{d\xi^4} + \frac{2(\chi_1^i+\chi_2^i)}{\xi}\frac{d^3}{d\xi^3} - \frac{(1+2n^2)(\chi_1^i+\chi_2^i)}{\xi^2}\frac{d^2}{d\xi^2}$$

$$+ \frac{(1+2n^2)(\chi_1^i+\chi_2^i)}{\xi^3}\frac{d}{d\xi} + \frac{(n^4-4n^2)(\chi_1^i+\chi_2^i)}{\xi^4}, \tag{31}$$

$$\chi_1^i = \frac{6xg^2(E_c-E_m)^2}{E_c(1+g)(2+g)^2[E_c(\psi+g\psi-2x)+E_m(\psi+g\psi-2xg)]}, \tag{32}$$

$$\chi_2^i = \frac{E_c[\psi(12+6g+6g^2)-\psi(1+g)(2+g)(3+g)]+E_m[\psi(16g+6g^2+2g^3)-\psi(1+g)(2+g)(3+g)]}{2\psi E_c(1+g)(2+g)(3+g)}, \tag{33}$$

$$\mu^i = \frac{(-g\psi-\psi+2x)-\frac{\rho_m}{\rho_c}(g\psi+\psi-2xg)}{2x(1+g)}, \tag{34}$$

$$\lambda = \omega R^2 \sqrt{\rho_c h / D_c}, \tag{35}$$

$$D_c = \frac{E_c h^3}{12(1-v^2)}. \tag{36}$$

The boundary conditions on the outer edge ($\xi = 1$) of the porous FGM circular plate may be one of the following: clamped, simply supported, sliding supported and free. These conditions may be written in terms of the radial mode function $W(\xi)$ in the following form:

- Clamped:

$$W(\xi)|_{\xi=1} = 0, \tag{37a}$$

$$\frac{dW}{d\xi}|_{\xi=1} = 0. \tag{37b}$$

- Simply supported:

$$W(\xi)|_{\xi=1} = 0, \tag{38a}$$

$$M(W)|_{\xi=1} = \left[\frac{d^2 W}{d\xi^2} + \frac{v}{\xi}\frac{dW}{d\xi} - \frac{v n^2}{\xi^2}W\right]_{\xi=1} = 0. \tag{38b}$$

- Sliding supported:

$$\frac{dW}{d\xi}|_{\xi=1} = 0, \tag{39a}$$

$$V(W)|_{\xi=1} = \left[\frac{d^3 W}{d\xi^3} + \frac{1}{\xi}\frac{d^2 W}{d\xi^2} - \left(\frac{1+2n^2-vn^2}{\xi^2}\right)\frac{dW}{d\xi} + \left(\frac{3n^2-vn^2}{\xi^3}\right)W\right]_{\xi=1} = 0, \tag{39b}$$

- Free:

$$M(W)|_{\xi=1} = 0, \tag{40a}$$

$$V(W)|_{\xi=1} = 0. \tag{40b}$$

The static forces $M(W)$ and $V(W)$ are the normalized radial bending moment and the normalized effective shear force, respectively.

6. Solution of the problem

The one multiparametric general solution of the defined differential equation (30) for FGM circular/annular plates with the two various types of distribution of porosities ($i = \{e, u\}$) is obtained in the following form:

$$W_n^i(\xi, \lambda, g, \psi) = C_1 J_n\left[\left(\lambda\sqrt{\mathfrak{M}_i}\right)^{1/2}\xi\right] + C_2 I_n\left[\left(\lambda\sqrt{\mathfrak{M}_i}\right)^{1/2}\xi\right] + C_3 Y_n\left[\left(\lambda\sqrt{\mathfrak{M}_i}\right)^{1/2}\xi\right] +$$
$$C_4 K_n\left[\left(\lambda\sqrt{\mathfrak{M}_i}\right)^{1/2}\xi\right], \tag{41}$$

where n ($n \in \mathbb{N}^+$) is the number of nodal lines, C_1, C_2, C_3, C_4 are the constants of integration, $J_n\left[\left(\lambda\sqrt{\mathfrak{M}_i}\right)^{1/2}\xi\right], I_n\left[\left(\lambda\sqrt{\mathfrak{M}_i}\right)^{1/2}\xi\right], Y_n\left[\left(\lambda\sqrt{\mathfrak{M}_i}\right)^{1/2}\xi\right], K_n\left[\left(\lambda\sqrt{\mathfrak{M}_i}\right)^{1/2}\xi\right]$ are the Bessel functions as particular solutions of Eq. (30), $\mathfrak{M}_i$ is the generalized multiparametric function defined as:

$$\mathfrak{M}_i \equiv \mathfrak{M}_i(x, y, g, \psi, E_m, E_c, \rho_m, \rho_c) = \frac{\Omega_1^i}{\Omega_2^i + \Omega_3^i}, \quad \mathfrak{M}_i \geq 1 \quad \forall g \in [0, \infty] \land \forall \psi \in [0,1), \tag{42}$$

where

$$\Omega_1^i = -E_c x(2+g)^2[\rho_c(g\psi + \psi - 2x) + \rho_m(g\psi + \psi - 2xg)], \tag{43a}$$

$$\Omega_2^i = \frac{12xyg^2(E_c - E_m)^2\rho_c}{E_c(g\psi + \psi - 2x) + E_m(g\psi + \psi - 2xg)}, \tag{43b}$$

$$\Omega_3^i = \frac{(2+g)\rho_c\left[E_c\left[y(12+6g+6g^2) - \psi(1+g)(2+g)(3+g)\right] + E_m\left[y(16g+6g^2+2g^3) - \psi(1+g)(2+g)(3+g)\right]\right]}{3+g}. \tag{43c}$$

The functions $J_n\left[\left(\lambda\sqrt{\mathfrak{M}_i}\right)^{1/2}\xi\right]$ and $I_n\left[\left(\lambda\sqrt{\mathfrak{M}_i}\right)^{1/2}\xi\right]$ are the limited linear independent solutions $\left(\lim_{\xi\to 0}J_n\left[\left(\lambda\sqrt{\mathfrak{M}_i}\right)^{1/2}\xi\right]<\infty,\ \lim_{\xi\to 0}I_n\left[\left(\lambda\sqrt{\mathfrak{M}_i}\right)^{1/2}\xi\right]<\infty\right)$ of Eq. (30) for the axisymmetric and non-axisymmetric deflections at center ($\xi=0$) of the porous FGM circular plate and diverse values of the physically justified parameters λ, g and ψ. The particular solutions $Y_n\left[\left(\lambda\sqrt{\mathfrak{M}_i}\right)^{1/2}\xi\right]$ and $K_n\left[\left(\lambda\sqrt{\mathfrak{M}_i}\right)^{1/2}\xi\right]$ are unlimited $\left(\lim_{\xi\to 0}Y_n\left[\left(\lambda\sqrt{\mathfrak{M}_i}\right)^{1/2}\xi\right]=-\infty,\ \lim_{\xi\to 0}K_n\left[\left(\lambda\sqrt{\mathfrak{M}_i}\right)^{1/2}\xi\right]=\infty\right)$ for the deflection at center of the plate, then the general solution (41) for the porous FGM circular plate can be presented in the new form:

$$W_n^i(\xi,\lambda,g,\psi)=C_1\Psi_1+C_2\Psi_2, \tag{44}$$

where

$$\Psi_1\equiv J_n\left[\left(\lambda\sqrt{\mathfrak{M}_i}\right)^{1/2}\xi\right], \tag{45a}$$

$$\Psi_2\equiv I_n\left[\left(\lambda\sqrt{\mathfrak{M}_i}\right)^{1/2}\xi\right]. \tag{45b}$$

By applying the general solution (44) and the boundary conditions (37÷40) as well as assuming the existence of the non-trivial constants C_1 and C_2, the general non-linear multiparametric characteristic equations of the FGM circular plate with the two various types of distribution of porosities were obtained in the form:

- Clamped (C):

$$\Delta_C^i(\lambda,g,\psi,n,x,y)\equiv\begin{vmatrix}\Psi_1 & \Psi_2\\ \frac{\partial\Psi_1}{\partial\xi} & \frac{\partial\Psi_2}{\partial\xi}\end{vmatrix}_{\xi=1}=0; \tag{46a}$$

- Simply supported (SS):

$$\Delta_{SS}^i(\lambda,g,\psi,n,x,y)\equiv\begin{vmatrix}\Psi_1 & \Psi_2\\ M[\Psi_1] & M[\Psi_2]\end{vmatrix}_{\xi=1}=0; \tag{46b}$$

- Sliding supported (S):

$$\Delta_S^i(\lambda,g,\psi,n,x,y)\equiv\begin{vmatrix}\frac{\partial\Psi_1}{\partial\xi} & \frac{\partial\Psi_2}{\partial\xi}\\ V[\Psi_1] & V[\Psi_2]\end{vmatrix}_{\xi=1}=0; \tag{46c}$$

- Free (F):

$$\Delta_F^i(\lambda,g,\psi,n,x,y)\equiv\begin{vmatrix}M[\Psi_1] & M[\Psi_2]\\ V[\Psi_1] & V[\Psi_2]\end{vmatrix}_{\xi=1}=0. \tag{46d}$$

If $x=y=1$ is introduced to Eqs. (42) and (45), then the obtained characteristic equations (46) will be valid for the FGM circular plates with even ($i=e$) distribution of porosities. If $x=2$, $y=4$ is introduced to Eqs. (42) and (45), than the obtained characteristic equations (46) will be valid for the FGM circular plates with uneven ($i=u$) distribution of porosities.

The general solution for the perfect (without porosity) FGM circular plate can be obtained from Eq. (44) and presented in the following form:

$$W_n(\xi,\lambda,g)\equiv\lim_{\psi\to 0}W_n^i(\xi,\lambda,g,\psi)=C_1\lim_{\psi\to 0}J_n\left[\left(\lambda\sqrt{\mathfrak{M}_i}\right)^{1/2}\xi\right]+C_2\lim_{\psi\to 0}I_n\left[\left(\lambda\sqrt{\mathfrak{M}_i}\right)^{1/2}\xi\right]. \tag{47}$$

After calculations, the final form of general solution for the perfect FGM circular plate is expressed as

$$W_n(\xi,\lambda,g)=J_n\left[\left(\lambda\sqrt{\mathfrak{D}}\right)^{1/2}\xi\right]+I_n\left[\left(\lambda\sqrt{\mathfrak{D}}\right)^{1/2}\xi\right], \tag{48}$$

where

$$\mathfrak{Y} = \frac{E_c(2+g)^2(3+g)(E_c+gE_m)(\rho_c+g\rho_m)}{\rho_c(1+g)[12E_c^2+(28g+16g^2+4g^3)E_cE_m+(7g^2+4g^3+g^4)E_m^2]}. \tag{49}$$

The general solution for the perfect FGM circular plate with negligible effect of the coupling in-plane and transverse displacements has the form:

$$W_n(\xi,\lambda,g) = C_1 J_n\left[\left(\lambda\sqrt{\mathfrak{P}}\right)^{1/2}\xi\right] + C_2 I_n\left[\left(\lambda\sqrt{\mathfrak{P}}\right)^{1/2}\xi\right], \tag{50}$$

where

$$\mathfrak{P} = \frac{E_c(2+g)(3+g)(\rho_c+g\rho_m)}{\rho_c[3E_c(2+g+g^2)+E_m(8g+3g^2+g^3)]}. \tag{51}$$

7. Parametric study

The every single fundamental and lower dimensionless frequencies of the free axisymmetric and non-axisymmetric vibrations of porous FGM circular plate were calculated for diverse values of the power-law index g, the porosity volume fraction ψ and different boundary conditions using the Newton method aided by calculation software MATHEMATICA v11.

The Poisson's ratio is taken as $\nu = 0.3$ and its variation is assumed to be negligible. In the present study, aluminum is taken as the metal and alumina is taken as the ceramic material. The values of Young's modulus and densities are taken as follows: $E_m = 70$ GPa, $E_c = 380$ GPa, $\rho_m = 2702$ kg/m^3, $\rho_c = 3800$ kg/m^3.

7.1. Imperfect FGM circular plate

The obtained numerical results for the first three dimensionless frequencies $\lambda = \omega R^2\sqrt{\rho_c h/D_c}$ of the axisymmetric $(n = 0)$ and non-axisymmetric $(n = 1)$ vibrations of the perfect $(\psi \to 0)$ homogeneous $(g \to 0)$ circular plate with various boundary conditions are presented in Table 1 and compared with the results obtained by Wu and Liu [36], Yalcin et al. [37], Zhou et al. [38], Duan et al. [39]. The obtained numerical results for the perfect homogeneous circular plate are in excellent agreement with those available in the literature.

Table 1. The dimensionless frequencies of the perfect homogeneous circular plate.

λ		Clamped		Simply supported		Sliding supported		Free	
					n				
		0	1	0	1	0	1	0	1
	Present	10.215	21.260	4.935	13.898	14.682	3.082	9.003	20.474
	[36]	10.216	21.260	4.935	13.898	14.682	3.082	9.003	20.475
λ_0	[37]	10.215	21.260	4.935	13.898	-	-	9.003	20.474
	[38]	10.215	21.260	4.935	13.898	-	-	9.003	20.474
	[39]	10.215	21.260	4.935	13.898	-	-	9.003	20.474
	Present	39.771	60.828	29.720	48.478	49.218	28.398	38.443	59.812
	[36]	39.771	60.829	29.720	48.478	49.218	28.399	38.443	59.812
λ_1	[37]	39.771	60.828	29.720	48.479	-	-	38.443	59.811
	[38]	39.771	60.828	29.720	48.478	-	-	38.443	59.811
	[39]	39.771	60.828	29.719	48.478	-	-	38.443	59.812
	Present	89.104	120.079	74.156	102.773	103.499	72.859	87.750	118.957
	[36]	89.104	120.079	74.156	102.772	103.499	72.859	87.750	118.957
λ_2	[37]	89.104	120.079	74.156	102.773	-	-	87.705	118.957
	[38]	89.104	120.080	74.156	102.773	-	-	87.750	118.957
	[39]	89.104	120.079	74.156	102.773	-	-	87.750	118.957

The calculated fundamental dimensionless frequencies λ_0 of the axisymmetric ($n = 0$) and non-axisymmetric ($n = 1$) vibrations of the FGM circular plate with evenly ($i = e$) and unevenly ($i = u$) distributed porosity are presented in Tables 2÷5. In the parametric study, values of the power-law index of FGMs is taken as $g = \{0, 0.2, 0.4, 0.6, 1, 2, 3, 4, 5\}$ and values of the porosity volume fraction is taken as $\psi = \{0, 0.05, 0.1, 0.2, 0.3\}$.

Table 2. The dimensionless fundamental frequencies of the clamped porous FGM circular plate.

i	n	ψ	g								
			0	0.2	0.4	0.6	1	2	3	4	5
			λ_0								
e	0	0	10.215	9.481	8.896	8.436	7.797	7.090	6.867	6.777	6.724
		0.05	10.286	9.522	8.905	8.414	7.718	6.920	6.661	6.559	6.503
		0.1	10.362	9.566	8.914	8.387	7.623	6.712	6.401	6.280	6.219
		0.2	10.535	9.668	8.932	8.315	7.374	6.113	5.612	5.402	5.305
		0.3	10.745	9.792	8.948	8.207	6.993	5.034	3.949	3.312	2.923
	1	0	21.260	19.731	18.514	17.557	16.228	14.756	14.292	14.105	13.993
		0.05	21.406	19.816	18.533	17.510	16.062	14.402	13.863	13.650	13.533
		0.1	21.564	19.909	18.552	17.454	15.866	13.968	13.222	13.069	12.942
		0.2	21.925	20.121	18.590	17.304	15.346	12.723	11.680	11.242	11.041
		0.3	22.362	20.380	18.622	17.081	14.554	10.478	8.220	6.894	6.084
u	0	0	10.215	9.481	8.896	8.436	7.797	7.090	6.867	6.777	6.724
		0.05	10.288	9.544	8.949	8.478	7.819	7.079	6.844	6.751	6.698
		0.1	10.364	9.611	9.004	8.521	7.840	7.065	6.816	6.719	6.666
		0.2	10.523	9.751	9.120	8.612	7.882	7.023	6.738	6.630	6.577
		0.3	10.696	9.903	9.246	8.710	7.923	6.959	6.622	6.495	6.438
	1	0	21.260	19.731	18.514	17.557	16.228	14.756	14.292	14.105	13.993
		0.05	21.411	19.864	18.624	17.644	16.272	14.733	14.244	14.050	13.940
		0.1	21.568	20.001	18.738	17.734	16.316	14.703	14.182	13.983	13.874
		0.2	21.901	20.293	18.980	17.923	16.404	14.617	14.023	13.798	13.688
		0.3	22.260	20.610	19.243	18.127	16.490	14.483	13.782	13.517	13.399

Table 3. The dimensionless fundamental frequencies of the simply supported porous FGM circular plate.

i	n	ψ	g								
			0	0.2	0.4	0.6	1	2	3	4	5
			λ_0								
e	0	0	4.935	4.580	4.297	4.075	3.767	3.425	3.317	3.274	3.248
		0.05	4.969	4.600	4.302	4.064	3.728	3.343	3.218	3.168	3.141
		0.1	5.005	4.621	4.306	4.051	3.683	3.242	3.092	3.033	3.004
		0.2	5.089	4.670	4.315	4.017	3.562	2.953	2.711	2.609	2.563
		0.3	5.190	4.730	4.322	3.965	3.378	2.432	1.908	1.600	1.412
	1	0	13.898	12.898	12.103	11.477	10.608	9.646	9.343	9.220	9.147
		0.05	13.993	12.954	12.115	11.446	10.500	9.415	9.062	8.923	8.847
		0.1	14.097	13.015	12.127	11.410	10.372	9.131	8.708	8.543	8.460
		0.2	14.333	13.153	12.152	11.312	10.032	8.317	7.635	7.349	7.218
		0.3	14.618	13.322	12.173	11.166	9.514	6.849	5.373	4.506	3.977
u	0	0	4.935	4.580	4.297	4.075	3.767	3.425	3.317	3.274	3.248
		0.05	4.970	4.611	4.323	4.095	3.777	3.420	3.306	3.261	3.236
		0.1	5.006	4.643	4.349	4.116	3.787	3.413	3.292	3.246	3.220
		0.2	5.083	4.710	4.406	4.160	3.808	3.393	3.255	3.203	3.177
		0.3	5.167	4.784	4.467	4.207	3.828	3.362	3.199	3.137	3.110
	1	0	13.898	12.898	12.103	11.477	10.608	9.646	9.343	9.220	9.147
		0.05	13.997	12.985	12.174	11.534	10.637	9.631	9.311	9.185	9.113
		0.1	14.099	13.075	12.249	11.592	10.666	9.611	9.273	9.141	9.069
		0.2	14.317	13.266	12.408	11.716	10.724	9.555	9.167	9.020	8.948
		0.3	14.551	13.473	12.580	11.850	10.780	9.468	9.009	8.836	8.759

Table 4. The dimensionless fundamental frequencies of the porous FGM circular plate with sliding support.

i	n	ψ	g								
			0	0.2	0.4	0.6	1	2	3	4	5
			λ_0								
e	0	0	14.682	13.626	12.785	12.124	11.206	10.190	9.870	9.740	9.663
		0.05	14.782	13.685	12.798	12.092	11.092	9.946	9.573	9.426	9.346
		0.1	14.892	13.749	12.811	12.053	10.956	9.646	9.199	9.025	8.938
		0.2	15.141	13.895	12.837	11.950	10.597	8.786	8.066	7.764	7.625
		0.3	15.442	14.074	12.860	11.796	10.051	7.236	5.676	4.761	4.201
	1	0	3.082	2.860	2.684	2.545	2.352	2.139	2.072	2.045	2.029
		0.05	3.103	2.873	2.687	2.538	2.328	2.088	2.010	1.980	1.962
		0.1	3.126	2.886	2.690	2.530	2.300	2.025	1.931	1.894	1.876
		0.2	3.178	2.917	2.695	2.509	2.225	1.844	1.693	1.630	1.600
		0.3	3.242	2.954	2.700	2.476	2.110	1.519	1.191	0.999	0.882
u	0	0	14.682	13.626	12.785	12.124	11.206	10.190	9.870	9.740	9.663
		0.05	14.786	13.717	12.861	12.184	11.237	10.174	9.836	9.703	9.627
		0.1	14.895	13.812	12.940	12.246	11.268	10.154	9.795	9.656	9.581
		0.2	15.124	14.014	13.107	12.377	11.328	10.094	9.684	9.529	9.453
		0.3	15.372	14.233	13.289	12.518	11.388	10.002	9.518	9.334	9.253
	1	0	3.082	2.860	2.684	2.545	2.352	2.139	2.072	2.045	2.029
		0.05	3.104	2.880	2.700	2.558	2.359	2.136	2.065	2.037	2.021
		0.1	3.127	2.890	2.716	2.571	2.365	2.131	2.056	2.027	2.011
		0.2	3.175	2.942	2.752	2.598	2.378	2.119	2.033	2.000	1.984
		0.3	3.227	2.988	2.790	2.628	2.391	2.100	1.998	1.960	1.942

Table 5. The dimensionless fundamental frequencies of the free porous FGM circular plate.

i	n	ψ	g								
			0	0.2	0.4	0.6	1	2	3	4	5
			λ_0								
e	0	0	9.003	8.355	7.840	7.435	6.872	6.248	6.052	5.973	5.926
		0.05	9.064	8.391	7.848	7.415	6.802	6.099	5.870	5.780	5.731
		0.1	9.132	8.431	7.856	7.391	6.718	5.915	5.641	5.534	5.480
		0.2	9.284	8.521	7.872	7.328	6.498	5.388	4.946	4.761	4.675
		0.3	9.469	8.630	7.886	7.233	6.163	4.437	3.481	2.919	2.576
	1	0	20.474	19.002	17.830	16.908	15.628	14.211	13.764	13.584	13.476
		0.05	20.615	19.084	17.848	16.863	15.468	13.870	13.350	13.145	13.033
		0.1	20.767	19.173	17.866	16.809	15.280	13.452	12.829	12.586	12.464
		0.2	21.115	19.378	17.902	16.665	14.779	12.253	11.248	10.827	10.633
		0.3	21.535	19.628	17.934	16.450	14.016	10.091	7.916	6.639	5.859
u	0	0	9.003	8.355	7.840	7.435	6.872	6.248	6.052	5.973	5.926
		0.05	9.067	8.411	7.886	7.471	6.890	6.239	6.032	5.950	5.903
		0.1	9.133	8.470	7.935	7.509	6.909	6.226	6.007	5.921	5.875
		0.2	9.274	8.593	8.037	7.590	6.947	6.190	5.938	5.843	5.796
		0.3	9.426	8.728	8.149	7.676	6.983	6.133	5.836	5.724	5.674
	1	0	20.474	19.002	17.830	16.908	15.628	14.211	13.764	13.584	13.476
		0.05	20.620	19.129	17.935	16.992	15.670	14.188	13.718	13.531	13.425
		0.1	20.771	19.262	18.045	17.078	15.713	14.160	13.660	13.466	13.361
		0.2	21.091	19.543	18.279	17.261	15.798	14.077	13.505	13.288	13.182
		0.3	21.437	19.848	18.532	17.457	15.881	13.948	13.273	13.017	12.903
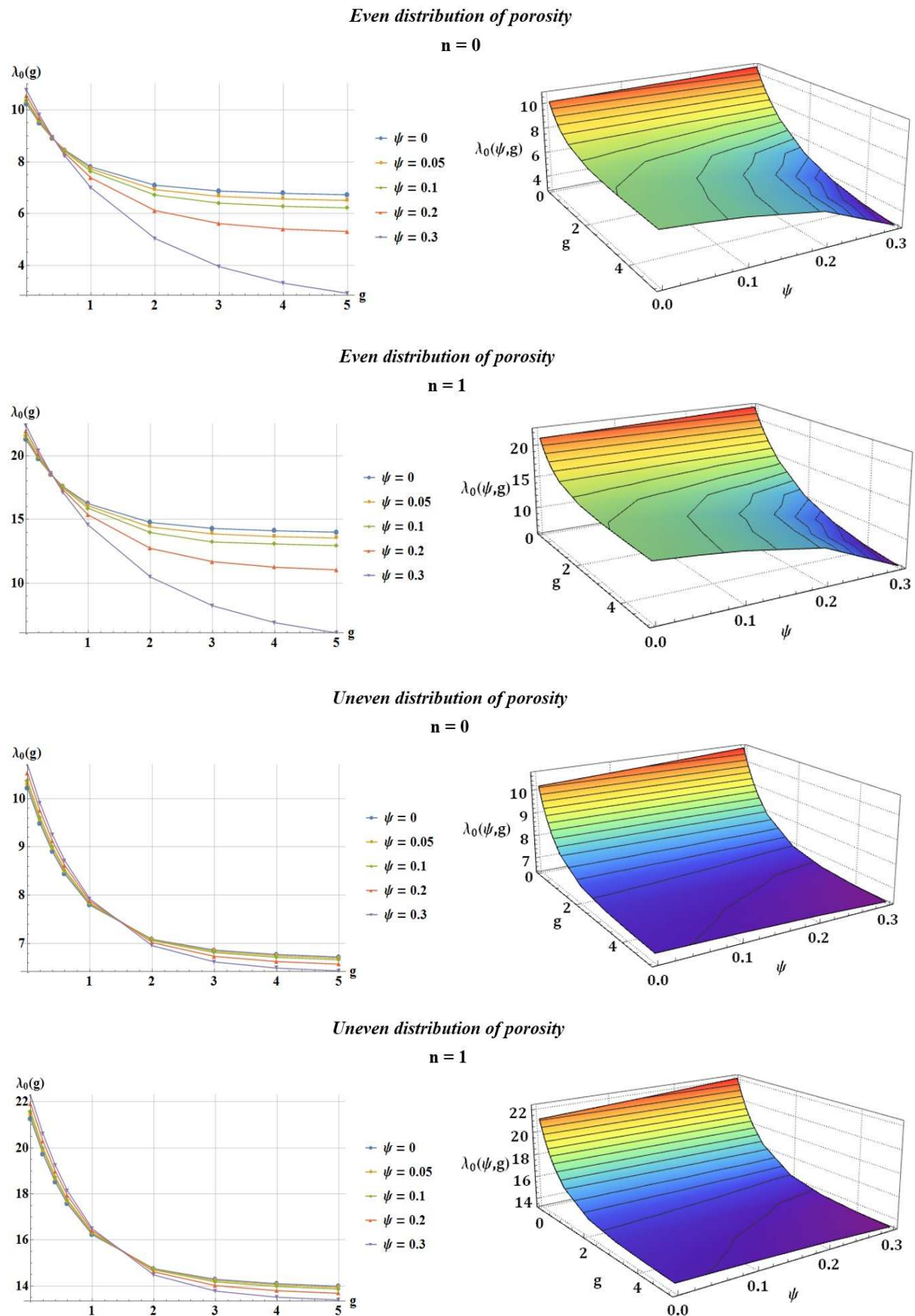
Fig. 3. The dependence of the fundamental dimensionless frequencies λ_0 of the free axisymmetric ($n = 0$) and non-axisymmetric ($n = 1$) vibrations on selected values of the power-law index and the porosity volume fraction of the clamped circular plate with evenly and unevenly distributed porosities.
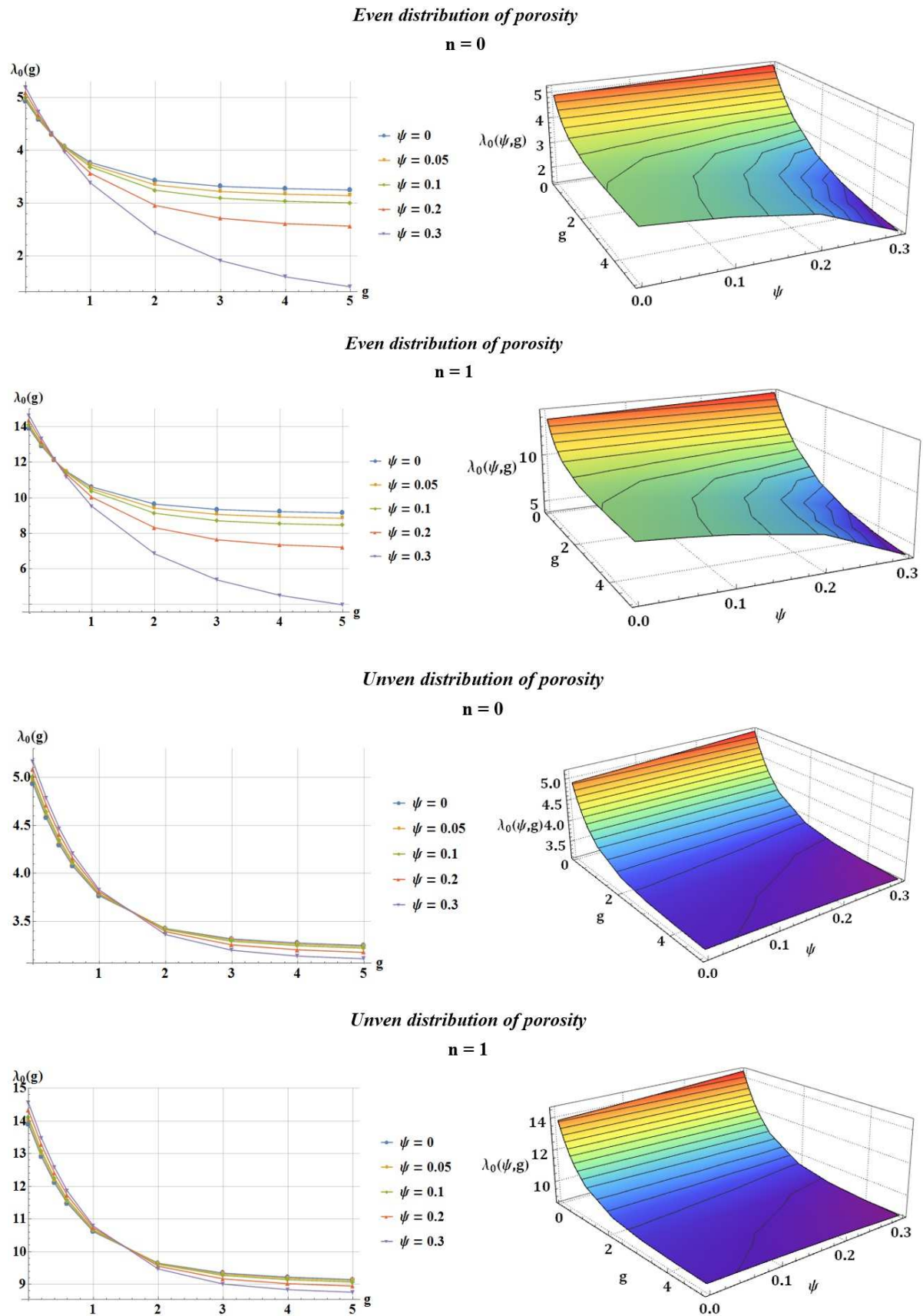
Fig. 4. The dependence of the fundamental dimensionless frequencies λ_0 of the free axisymmetric ($n = 0$) and non-axisymmetric ($n = 1$) vibrations on selected values of the power-law index and the porosity volume fraction of the simply supported circular plate with evenly and unevenly distributed porosities.
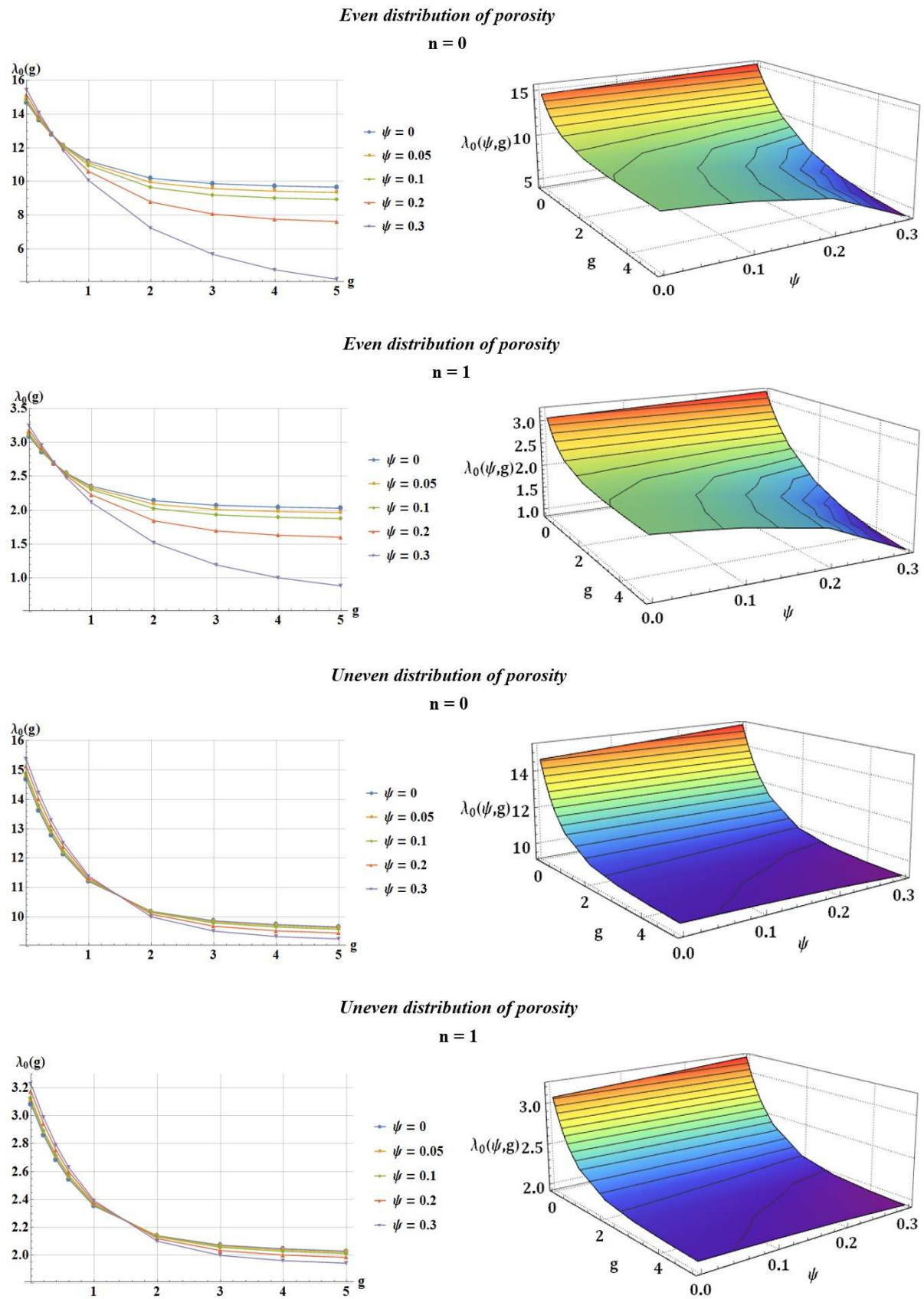
Fig. 5. The dependence of the fundamental dimensionless frequencies λ_0 of the free axisymmetric $(n = 0)$ and non-axisymmetric $(n = 1)$ vibrations on selected values of the power-law index and the porosity volume fraction of the sliding supported circular plate with evenly and unevenly distributed porosities.
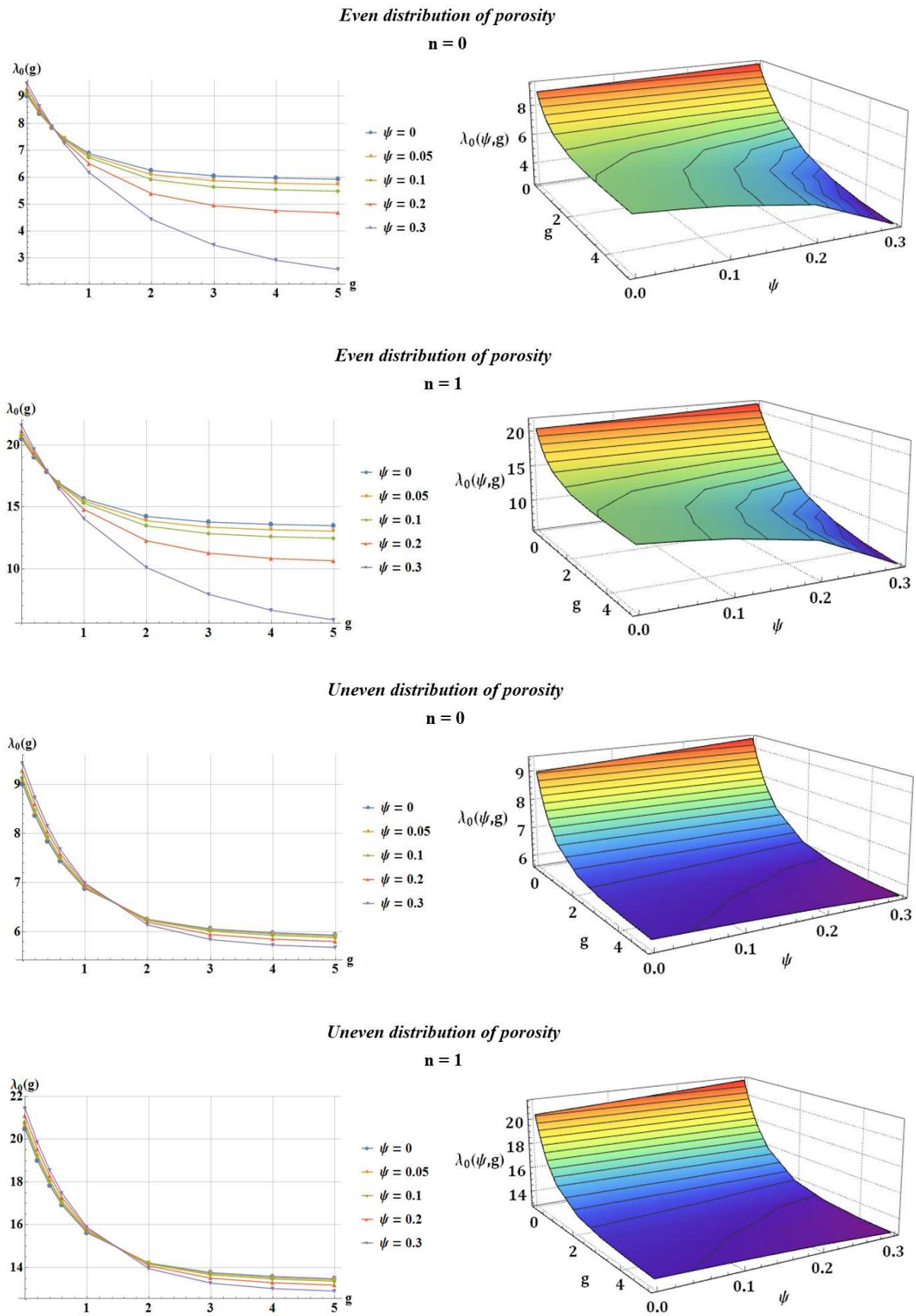
Fig. 6. The dependence of the fundamental dimensionless frequencies λ_0 of the free axisymmetric $(n = 0)$ and non-axisymmetric $(n = 1)$ vibrations on selected values of the power-law index and the porosity volume fraction of the free circular plate with evenly and unevenly distributed porosities.

The dependences of the fundamental dimensionless frequencies λ_0 of the free axisymmetric ($n = 0$) and non-axisymmetric ($n = 1$) vibrations of the circular plate on selected values of the power-law index and the porosities volume fraction are presented in Figures 3÷6 as the two-dimensional (2D) and three-dimensional (3D) graphs for the two various types of distribution of porosity and all considered boundary conditions.

7.2. Perfect FGM circular plate

The obtained general solution (48) and the defined boundary conditions (37÷40) were used to calculate the first three dimensionless frequencies λ of the axisymmetric ($n = 0$) and non-axisymmetric ($n = 1$) vibrations of the perfect ($\psi = 0$) FGM circular plate with various boundary conditions.

Table 6. The dimensionless frequencies of the clamped perfect FGM circular plate.

n	λ		g					
			1	2	3	4	5	∞
	λ_0	Present	7.797	7.090	6.867	6.777	6.724	5.199
		[28]	8.498	8.123	7.911	7.733	7.573	-
		[30]	8.498	8.123	7.911	7.733	7.573	5.199
0	λ_1	Present	30.357	27.604	26.737	26.386	26.177	20.243
		[28]	33.086	31.625	30.798	30.107	29.485	-
		[30]	33.086	31.625	30.798	30.107	29.485	20.243
	λ_2	Present	68.012	61.845	59.902	59.116	58.649	45.352
		[28]	74.127	70.855	69.002	67.453	66.059	-
		[30]	74.127	70.855	69.002	67.453	66.059	45.352
	λ_0	Present	16.228	14.756	14.292	14.105	13.993	10.821
		[30]	17.687	16.906	16.464	16.094	15.762	10.821
1	λ_1	Present	46.430	42.219	40.893	40.357	40.038	30.961
		[30]	50.604	48.370	47.105	46.048	45.097	30.961
	λ_2	Present	91.655	83.344	80.725	79.667	79.037	61.118
		[30]	99.896	95.486	92.989	90.901	89.024	61.118

Table 7. The dimensionless frequencies of the simply supported perfect FGM circular plate.

n	λ		g					
			1	2	3	4	5	∞
	λ_0	Present	3.767	3.425	3.317	3.274	3.248	2.512
		[28]	4.105	3.924	3.821	3.736	3.658	-
		[30]	4.105	3.924	3.821	3.736	3.658	2.512
0	λ_1	Present	22.685	20.628	19.980	19.717	19.562	15.127
		[28]	24.724	23.633	23.015	22.498	22.033	-
		[30]	24.724	23.633	23.015	22.498	22.033	15.127
	λ_2	Present	56.602	51.470	49.853	49.199	48.810	37.744
		[28]	61.692	58.968	57.426	56.137	54.977	-
		[30]	61.692	58.968	57.426	56.137	54.977	37.744
	λ_0	Present	10.608	9.646	9.343	9.220	9.147	7.074
		[30]	11.562	11.051	10.762	10.521	10.303	7.074
1	λ_1	Present	37.003	33.648	32.591	32.163	31.909	24.675
		[30]	40.330	38.550	37.542	36.699	35.941	24.675
	λ_2	Present	78.446	71.332	69.091	68.185	67.646	52.310
		[30]	85.499	81.724	79.587	77.801	76.194	52.310

The obtained numerical results are presented in Tables 6÷9 for selected values of the power-law index g. Numerical results obtained for the clamped and simply supported plates (Table 6 and Table 7) were compared with the results presented in previous papers [28, 30], where effect of the coupling in-plane and transverse displacements was omitted.

The fundamental dimensionless frequencies of the perfect FGM circular plates with and without effect of the coupling in-plane and transverse displacements obtained for selected values of the power-law index and diverse boundary conditions are presented in Table 10. Additionally, the differences (errors) between obtained results were calculated according to the equation:

$$\delta(\%) = \left(\frac{\lambda_0^{\mathfrak{P}} - \lambda_0^{\mathfrak{Y}}}{\lambda_0^{\mathfrak{P}}}\right) \cdot 100\%, \tag{52}$$

where $\lambda_0^{\mathfrak{P}}$ and $\lambda_0^{\mathfrak{Y}}$ are the fundamental dimensionless frequencies of the perfect FGM circular plate without and with effect of the coupling in-plane and transverse displacements, respectively. Figure 7 presents the dependence of the differences (errors) between obtained results for the power-law index $g \geq 0$.

Table 8. The dimensionless frequencies of the free perfect FGM circular plate.

n	λ	g					
		1	2	3	4	5	∞
0	λ_0	6.872	6.248	6.052	5.973	5.926	4.582
	λ_1	29.343	26.682	25.844	25.505	25.303	19.567
	λ_2	66.979	60.905	58.992	58.218	57.757	44.663
1	λ_0	15.628	14.211	13.764	13.584	13.476	10.421
	λ_1	45.653	41.513	40.209	39.682	39.368	30.443
	λ_2	90.799	82.565	79.971	78.922	78.298	60.547

Table 9. The dimensionless frequencies of the perfect FGM circular plate with sliding support.

n	λ	g					
		1	2	3	4	5	∞
0	λ_0	11.206	10.190	9.870	9.740	9.663	7.473
	λ_1	37.568	34.161	33.088	32.654	32.396	25.051
	λ_2	79.000	71.836	69.579	68.667	68.124	52.680
1	λ_0	2.352	2.139	2.072	2.045	2.029	1.568
	λ_1	21.676	19.711	19.091	18.841	18.692	14.454
	λ_2	55.612	50.569	48.981	48.338	47.956	37.084
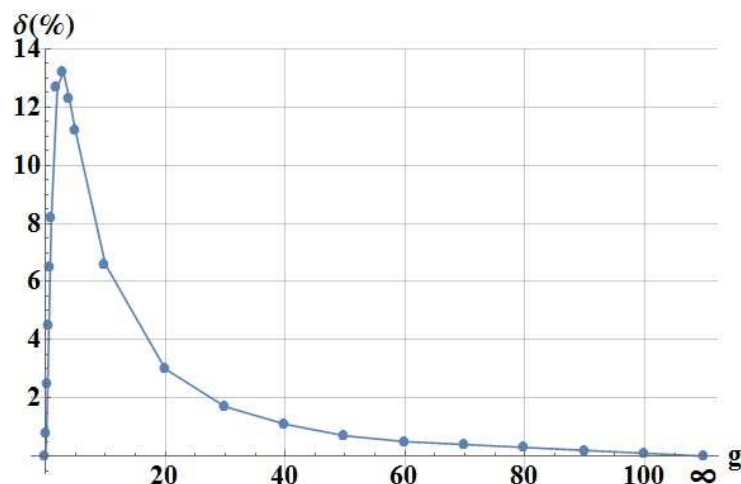
Fig. 7. The dependence of the differences (errors) between the fundamental dimensionless frequencies of the perfect FGM circular plate without ($\lambda_0^{\mathfrak{P}}$) and with ($\lambda_0^{\mathfrak{Y}}$) effect of the coupling in-plane and transverse displacements for diverse values of the power-law index.

Table 10. The differences between the fundamental dimensionless frequencies of the perfect FGM circular plates with and without effect of the coupling in-plane and transverse displacements.

BCs	n	λ	g								
			1	2	3	4	5	10	30	60	∞
Clamped	0	$\lambda_0^{\mathfrak{P}}$	8.498	8.123	7.911	7.733	7.573	6.977	6.064	5.687	5.199
		$\lambda_0^{\mathfrak{D}}$	7.797	7.090	6.867	6.777	6.724	6.512	5.960	5.654	5.199
		$\delta(\%)$	**8.2**	**12.7**	**13.2**	**12.3**	**11.2**	**6.6**	**1.7**	**0.5**	**0**
	1	$\lambda_0^{\mathfrak{P}}$	17.687	16.906	16.464	16.094	15.762	14.520	12.621	11.835	10.821
		$\lambda_0^{\mathfrak{D}}$	16.228	14.756	14.292	14.105	13.993	13.552	12.404	11.767	10.821
		$\delta(\%)$	**8.2**	**12.7**	**13.2**	**12.3**	**11.2**	**6.6**	**1.7**	**0.5**	**0**
Simply supported	0	$\lambda_0^{\mathfrak{P}}$	4.105	3.924	3.821	3.736	3.658	3.370	2.929	2.747	2.512
		$\lambda_0^{\mathfrak{D}}$	3.767	3.425	3.317	3.274	3.248	3.145	2.879	2.731	2.512
		$\delta(\%)$	**8.2**	**12.7**	**13.2**	**12.3**	**11.2**	**6.6**	**1.7**	**0.5**	**0**
	1	$\lambda_0^{\mathfrak{P}}$	11.562	11.051	10.762	10.521	10.303	9.492	8.250	7.737	7.074
		$\lambda_0^{\mathfrak{D}}$	10.608	9.646	9.343	9.220	9.147	8.859	8.108	7.692	7.074
		$\delta(\%)$	**8.2**	**12.7**	**13.2**	**12.3**	**11.2**	**6.6**	**1.7**	**0.5**	**0**
Sliding supported	0	$\lambda_0^{\mathfrak{P}}$	12.214	11.675	11.369	11.114	10.885	10.027	8.716	8.173	7.473
		$\lambda_0^{\mathfrak{D}}$	11.206	10.190	9.870	9.740	9.663	9.359	8.566	8.126	7.473
		$\delta(\%)$	**8.2**	**12.7**	**13.2**	**12.3**	**11.2**	**6.6**	**1.7**	**0.5**	**0**
	1	$\lambda_0^{\mathfrak{P}}$	2.564	2.451	2.387	2.333	2.285	2.105	1.830	1.716	1.569
		$\lambda_0^{\mathfrak{D}}$	2.352	2.139	2.072	2.045	2.029	1.964	1.798	1.706	1.569
		$\delta(\%)$	**8.2**	**12.7**	**13.2**	**12.3**	**11.2**	**6.6**	**1.7**	**0.5**	**0**
Free	0	$\lambda_0^{\mathfrak{P}}$	7.489	7.159	6.972	6.815	6.674	6.149	5.344	5.012	4.582
		$\lambda_0^{\mathfrak{D}}$	6.872	6.248	6.052	5.973	5.926	5.739	5.252	4.983	4.582
		$\delta(\%)$	**8.2**	**12.7**	**13.2**	**12.3**	**11.2**	**6.6**	**1.7**	**0.5**	**0**
	1	$\lambda_0^{\mathfrak{P}}$	17.033	16.281	15.855	15.499	15.179	13.984	12.155	11.398	10.421
		$\lambda_0^{\mathfrak{D}}$	15.628	14.211	13.764	13.584	13.476	13.051	11.945	11.332	10.421
		$\delta(\%)$	**8.2**	**12.7**	**13.2**	**12.3**	**11.2**	**6.6**	**1.7**	**0.5**	**0**

8. Discussion

8.1. Imperfect FGM circular plate

The numerical results for the fundamental dimensionless frequencies of the porous FGM circular plates presented in Tables (2÷5) and Figures (3÷6) show the following dependences:

- the fundamental eigenfrequency λ_0 of the axisymmetric and non-axisymmetric vibrations of the circular plate decreases with the increasing value of the power-law index g for the two considered distributions of porosities and all considered values of the porosity volume fraction ψ;
- for the evenly distributed porosities, the fundamental eigenfrequency λ_0 of the axisymmetric and non-axisymmetric vibrations of the plate increases with the increasing value of the porosity volume fraction ψ for $g \in [0, 0.4]$ and decreases for $g \in [0.6, 5]$;
- for the unevenly distributed porosities, the fundamental eigenfrequency λ_0 of the axisymmetric and non-axisymmetric vibrations of the plate increases with the increasing value of the porosity volume fraction ψ for $g \in [0, 1]$ and decreases for $g \in [2, 5]$;
- the influence of values of the porosity volume fraction ψ on the values of the fundamental eigenfrequency λ_0 of the axisymmetric and non-axisymmetric vibrations of the plate is smaller for the unevenly distributed porosities than for the evenly distributed porosities;

- for the evenly distributed porosities, the fundamental eigenfrequency λ_0 of the axisymmetric and non-axisymmetric vibrations of plate decreases faster for $\psi = 0.3$ with the increasing values of the power-law index g than for $\psi = \{0, 0.1, 0.2\}$;
- for the unevenly distributed porosities, the fundamental eigenfrequency λ_0 of the axisymmetric and non-axisymmetric vibrations of the plate decreases slowly with the increasing values of the power-law index g for all considered values of the porosity volume fraction ψ.

The observed dependences exist because of the diverse influence of porosity distributions, values of the power-law index and the porosity volume fraction on decreasing (increasing) the ratios of mass to stiffness of the considered circular plates. The all observed dependences are independent of the considered boundary conditions which influence only the values of the dimensionless frequencies of the plate.

8.2. Perfect FGM circular plate

It can be observed that the values of dimensionless frequencies of the perfect FGM circular plates obtained by omitting the effect of coupling in-plane and transverse displacements are higher than the values of the dimensionless frequencies of the considered plate with the coupling effect. The differences (errors) between the calculated dimensionless frequencies of free axisymmetric and non-axisymmetric vibration of the perfect FGM circular plate with and without the coupling effect are significant for the power-law index $g \in [0, 20]$, but for $g \in [20, \infty]$ these differences decrease from 2% to 0%. It can be observed from Table 10 that the differences between the calculated dimensionless frequencies are independent of the modes of vibration and the boundary conditions of the considered circular plate.

9. Conclusions

This paper presents the influence of two different types of distribution of porosities on the free vibrations of the thin functionally graded circular plate with clamped, simply supported, sliding supported, and free edges. To this aim the boundary value problem was formulated and a solution was obtained in the exact form. The universal multiparametric characteristic equations were defined using the properties of the multiparametric general solution obtained for the plate with even and uneven distribution of porosities. The effects of the power-law index, the volume fraction index and diverse boundary conditions on the values of the dimensionless frequencies of the free axisymmetric and non-axisymmetric vibrations of the circular plate were comprehensively studied. Additionally, the influences of the power-law index and different boundary conditions on the values of dimensionless frequencies of the FGM circular plate without porosities were also presented.

The obtained multiparametric general solution will allow to study the influences of diverse additional complicating effects such as stepped thickness, cracks, additional mounted elements expressed by only additional boundary conditions on the dynamic behavior of the porous functionally graded circular and annular plates. The exact frequencies of vibration presented in non-dimensional form can serve as benchmark values for researchers and engineers to validate their analytical and numerical methods applied in design and analysis of porous functionally graded structural elements.

Acknowledgements

The research was conducted within S/WZ/1/2017 project and was financed by the funds of the Ministry of Science and Higher Education, Poland.

References

1. J. Zhu, Z. Lai, Z. Yin, J. Jeon, S. Lee, Fabrication of ZrO_2-NiCr functionally graded material by powder metallurgy, Materials Chemistry and Physics 68 (2001) 130-135.
2. N. Wattanasakulpong, B.G. Prusty, D.W. Kelly, M. Hoffman, Free vibration analysis of layered functionally graded beams with experimental validation, Materials and Design 36 (2012) 182-190.
3. M. Jabbari, E. Farzaneh Joubaneh, A.R. Khorshidvand, M.R. Eslami, Buckling analysis of porous circular plate with piezoelectric actuator layers under uniform radial compression, International Journal of Mechanical Sciences 70 (2013) 50-56.
4. A.R. Khorshidvand, E. Farzaneh Joubaneh, M. Jabbari, M.R. Eslami, Buckling analysis of a porous circular plate with piezoelectric sensor-actuator layers under uniform radial compression, Acta Mechanica 225 (2014) 179-193.
5. A. Mojahedin, E. Farzaneh Joubaneh, M. Jabbari, Thermal and mechanical stability of a circular porous plate with piezoelectric actuators, Acta Mechanica 225 (2014) 3437-3452.
6. A. Behravan Rad, M. Shariyat, Three-dimensional magneto-elastic analysis of asymmetric variable thickness porous FGM circular plates with non-uniform tractions and Kerr elastic foundations, Composite Structures 125 (2015) 558-574.
7. M.R. Barati, M.H. Sadr, A.M. Zenkour, Buckling analysis of higher order graded smart piezoelectric plates with porosities resting on elastic foundation, International Journal of Mechanical Sciences 117 (2016) 309-320.
8. I. Mechab, B. Mechab, S. Benaissa, B. Serier, B. Bachir Bouiadjra, Free vibration analysis of FGM nanoplate with porosities resting on Winkler Pasternak elastic foundations based on two-variable refined plate theories, Journal of the Brazilian Society of Mechanical Sciences and Engineering 38 (2016) 2193-2211.
9. A. Mojahedin, M. Jabbari, A.R. Khorshidvand, M.R. Eslami, Buckling analysis of functionally graded circular plates made of saturated porous materials based on higher order shear deformation theory, Thin-Walled Structures 99 (2016) 83-90.
10. Y.Q. Wang, J.W. Zu, Vibrations behaviors of functionally graded rectangular plates with porosities and moving in thermal environment, Aerospace Science and Technology 69 (2017) 550-562.
11. A. Gupta, M. Talha, Influence of porosity on the flexural and vibration response of gradient plate using nonpolynomial higher-order shear and normal deformation theory, International Journal of Mechanics and Materials in Design (2017) https://doi.org/10.1007/s10999-017-9369-2
12. Y.Q. Wang, J.W. Zu, Vibration characteristics of moving sigmoid functionally graded plates containing porosities, International Journal of Mechanics and Materials in Design (2017) https://doi.org/10.1007/s10999-017-9385-2
13. F. Ebrahimi, A. Jafari, M.R. Barati. Free vibration analysis of smart porous plates subjected to various physical fields considering neutral surface position, Arabian Journal for Science and Engineering 42 (2017) 1865-1881.
14. M.R. Feyzi, A.R. Khorshidvand, Axisymmetric post-buckling behavior of saturated porous circular plates, Thin-Walled Structures 112 (2017) 149-158.
15. Y.Q. Wang, J.W. Zu, Large-amplitude vibration of sigmoid functionally graded thin plates with porosities, Thin-Walled Structures 119 (2017) 911-924.
16. Y.Q. Wang, Y.H. Wan, Y.F. Zhang, Vibrations of longitudinally travelling functionally graded material plates with porosities, European Journal of Mechanics A/Solids 66 (2017) 55-68.
17. F. Ebrahimi, A. Jafari, M.R. Barati, Vibration analysis of magneto-electro-elastic heterogeneous porous material plates resting on elastic foundations, Thin-Walled Structures 119 (2017) 33-46.
18. H. Shahverdi, M.R. Barati, Vibration analysis of porous functionally graded nanoplates, International Journal of Engineering Science 120 (2017) 82-99.
19. M.H. Shojaeefard, H.S. Googarchin, M. Ghadiri, M. Mahinzare, Micro temperature-dependent FG porous plate: Free vibration and thermal buckling analysis using modified couple stress theory with CPT and FSDT, Applied Mathematical Modelling 50 (2017) 633-655.
20. M.R. Barati, H. Shahverdi, Nonlinear vibration of nonlocal four-variable graded plates with porosities implementing homotopy perturbation and Hamiltonian methods, Acta Mechanica 229 (2018) 343-362.
21. M.C. Kiran, S.C. Kattimani, M. Vinyas, Porosity influence on structural behaviour of skew functionally graded magneto-electro-elastic plate, Composite Structures 191 (2018) 36-77.

22. P.H. Cong, T.K. Chien, N.D. Khoa, N.D. Duc, Nonlinear thermomechanical buckling and post-buckling response of porous FGM plates using Reddy's HSDT, Aerospace Science and Technology 77 (2018) 419-428.

23. M.C. Kiran, S.C. Kattimani, Assessment of porosity influence on vibration and static behaviour of functionally graded magneto-electro-elastic plate: A finite element study, European Journal of Mechanics A/Solids 71 (2018) 258-277.

24. E. Arshid, A.R. Khorshidvand, Free vibration analysis of saturated porous FG circular plates integrated with piezoelectric actuators via differential quadrature method, Thin-Walled Structures 125 (2018) 220-233.

25. D. Shahsavari, M. Shahsavari, L. Li, B. Karami, A novel quasi-3D hyperbolic theory for free vibration of FG plates with porosities resting on Winkler/Pasternak/Kerr foundation, Aerospace Science and Technology 72 (2018) 134-149.

26. D-G. Zhang, Y-H. Zhou, A theoretical analysis of FGM thin plates based on physical neutral surface, Computational Materials Science 44 (2008) 716-720.

27. F. Ebrahimi, A. Rastgo, An analytical study on the free vibration of smart circular thin FGM plate based on classical plate theory, Thin-Walled Structures 46 (2008) 1402-1408.

28. R. Lal, N. Ahlawat, Axisymmetric vibrations and buckling analysis of functionally graded circular plates via differential transform method, European Journal of Mechanics A/Solids 52 (2015) 85-94.

29. R. Lal, N. Ahlawat, Buckling and vibration of functionally graded non-uniform circular plates resting on Winkler foundation, Latin American Journal of Solids and Structures 12 (2015) 2231-2258.

30. K.K. Żur, Quasi-Green's function approach to free vibration analysis of elastically supported functionally graded circular plates, Composite Structures 183 (2018) 600-610.

31. S. Abrate, Functionally graded plates behave like homogenous plates, Composites Part B 39 (2008) 151-158.

32. J.N. Reddy, C.M. Wang, S. Kitipornchai, Axisymmetric bending of functionally graded circular and annular plates, European Journal of Mechanics A/Solids 18 (1999) 185-199.

33. N. Wattanasakulong, A. Chaikittiratana, Flexural vibration of imperfect functionally graded beams based on Timoshenko beam theory: Chebyshev collocation method, Meccanica 50 (2015) 1331-1342.

34. F. Delale, F. Erdogan, The crack problem for a non-homogeneous plane, ASME Journal of Applied Mechanics 50 (1983) 609-614.

35. J.N. Reddy, Theory and analysis of elastic plates and shells, CRC Press (2006).

36. T.Y. Wu, G.R. Liu, Free vibration analysis of circular plates using generalized differential quadrature rule, Computer Methods in Applied Mechanics and Engineering 191 (2002) 5365-5380.

37. H.S. Yalcin, A. Arikoglu, I. Ozkol, Free vibration analysis of circular plates by differential transformation method, Applied Mathematics and Computation 212 (2009) 377-386.

38. Z.H. Zhou, K.W. Wong, X.S. Xu, A.Y.T. Leung, Natural vibration of circular and annular thin plates by Hamiltonian approach, Journal of Sound and Vibration 330 (2011) 1005-1017.

39. G. Duan, X. Wang, Ch. Jin, Free vibration analysis of circular thin plates with stepped thickness by the DSC element method, Thin-Walled Structures 85 (2014) 25-33.